

# Probes and Monitors for the Study of Solidification of Molten Semiconductors

Principal Investigator: Professor D.R. Sadoway

MJ 710807

## Abstract

Product morphology in metal casting and semiconductor crystal growth is strongly influenced by the nature of the solid-liquid interface during solidification. Since *in situ* observation of solidification in these technologically important systems is not possible, investigators have resorted to the use of physical models, such as water and organic liquids, which while they are transparent to visible light, suffer from the fact that their Prandtl numbers are too high. Molten alkali halides are better physical models in this respect, and are transparent to visible light. The purpose of the present study is to examine solidification in the LiCl-KCl system to determine if phenomena such as solute rejection can be observed by laser schlieren imaging.

## Introduction

The properties and performance of a material are determined by its structure and composition, both of which are to a large extent controlled through processing. In semiconductor crystal growth, for example, product morphology and dopant concentration are strongly influenced by the behavior of the solid-liquid interface during solidification, yet it is difficult to observe directly. Accordingly, it is necessary to resort to mathematical models and physical models must be chosen with a high degree of similarity to the system of interest, i.e., Prandtl number, Jackson  $\alpha$  factor, etc. Significant deviations in such properties from those of the system of interest can weaken the physical model to the extent that it cannot be assumed that certain phenomena observed in the model occur at all in the real system. This is particularly true for nontrivial solidification processes, such as solute redistribution in a multicomponent system. As another example, the problem of dendrite growth in metals has long been the subject of study. Many theories have been enunciated [1, 2, 3,]; however, it is extremely difficult to test them. Since *in situ* observation of solidification in molten metals is not possible, investigators have used physical models such as water and organic liquids, which are transparent to visible light. Table I compares the physical properties of several melts of technological significance to those of various analogs. Metals and elemental semiconductors have low Prandtl numbers ( $Pr < 10^{-2}$ ), while water and organic liquids have high Prandtl numbers ( $Pr > 10$ ). In the solidification of elemental semiconductors, the Jackson  $\alpha$  factor (approximated here as  $\Delta H_{\text{fusion}}/RT_{\text{melting}}$  and designated  $\mu$ ) is greater than 2, while in the solidification of many organic liquids  $\mu < 2$ . Such disparities in the Prandtl number and  $\mu$  are unacceptable for the reasons given above.

With these considerations in mind, the present study has turned to the use of molten alkali chlorides as physical models representative of systems of commercial interest.

Table 1. Physical Properties of Selected Liquids

Property	Cu	Si	H <sub>2</sub> O	SCN	KCl-LiCl
molecular weight (g mol <sup>-1</sup> )	63.55	28.09	18	80.09	55.47
melting temp, T <sub>mp</sub> (°C)	1083	1412	0	58.08	355
heat of fusion, ΔH <sub>f</sub> (J mol <sup>-1</sup> )	13,050	50,550	6008	3700	13,083
$\mu = \frac{\Delta H_f}{RT_{mp}}$	1.18	3.58	2.65	1.41	2.71-3.06
viscosity, η (Pa·s) × 10 <sup>3</sup>	4.0	1	1.787	4.6	1.46
thermal conductivity, κ <sub>th</sub> (Wm <sup>-1</sup> K <sup>-1</sup> )	165.6	31	0.561	0.223	0.6903
density, ρ (kg m <sup>-3</sup> )	8000	2520	1000	970	1577
heat capacity, C <sub>p</sub> (J mol <sup>-1</sup> K <sup>-1</sup> )	31.46	26.12	75.91	160	72.31
Prandtl Number *	1.2 × 10 <sup>-2</sup>	3 × 10 <sup>-2</sup>	> 13	41	< 6
crystal structure	fcc	diamond	hexagonal	bcc	sc

\* computed at T<sub>mp</sub>.

## The Present Study

As part of an investigation of the use of molten salts as physical models in solidification processes, fluid flow patterns in the melt are being studied by laser schlieren imaging.

Figure 1 is a schematic of the experimental apparatus. The salt melt is contained in a fused quartz cell which has a square cross-section, 2" on edge. The cell is set inside an electrical resistance furnace with two viewing ports. A water cooled copper chill makes contact with the cell wall along one side. Schlieren imaging is accomplished through the use of a 5 mW helium-neon laser. The initial 0.8 mm diameter beam is expanded to 22 mm diameter before entering the cell. A lens focuses the light leaving the cell. At the focal point there is a removable knife edge mounted on an x-y-z translator. A 35 mm camera body is positioned so that its film plane coincides with the image plane of the cell. Finally, a thin, straight wire is interposed between the laser source and the cell to act as a reference against which differences in index of refraction can be viewed.

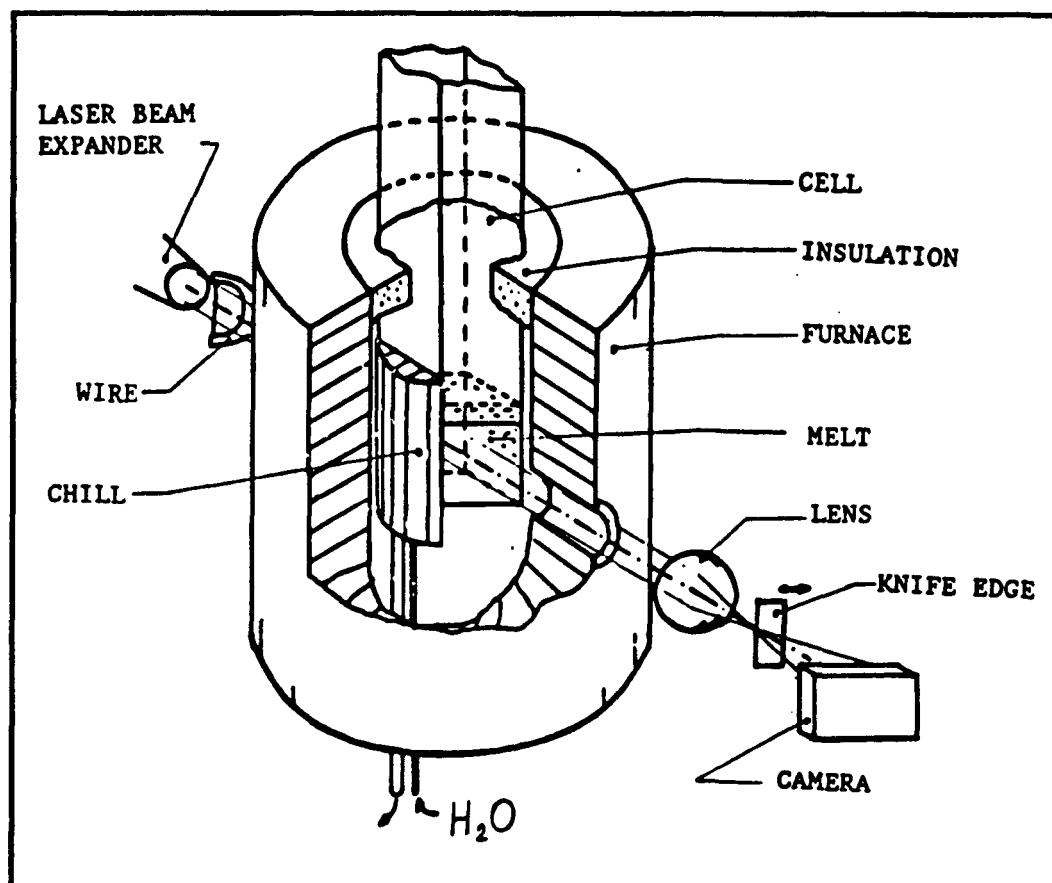


Figure 1. Schematic drawing of the experimental set-up.

In a typical experiment the purified salts are charged and melted in the cell. Then cooling water is fed to the chill and the resulting convection patterns are observed.

Two melt compositions have been chosen both in the LiCl-KCl system: the eutectic (41.5 mole% KCl) and an off-eutectic solution (46.2 mole% KCl).

Figure 2 shows a laser shadowgraph image of solidification of the eutectic melt. In a shadowgraph the schlieren knife edge has been removed from the light path. The chill plate is to the right of the field of view. Growth of solid phase is occurring in two directions: top down and bottom up. Dendrites near the cell wall are faceted; interior dendrites are not. Instead, they are thinner with multiple branches which sometimes broke off and fell (see Fig. 2(a)). Weak convective motion could be detected by schlieren imaging as seen in Figure 3.

Figures 4 and 5 show images selected during the solidification of the off-eutectic melt. The process was different in this example. First, there was only one growth direction, horizontally outward from the chill. Secondly, turbulent convection was observed. The general behavior of the schlieren images can be characterized as horizontal, wavelike motion at a frequency of  $\sim 0.5$  Hz. The source of these oscillations is presumed to be double diffusive instability. Since denser KCl is crystallizing the colder liquid close to the solid-liquid interface is richer in the less dense LiCl. Initially, the temperature effect on density dominates and the melt sinks. However, it appears that heat transfer is more rapid than mass transfer: the melt temperature rises and the compositional

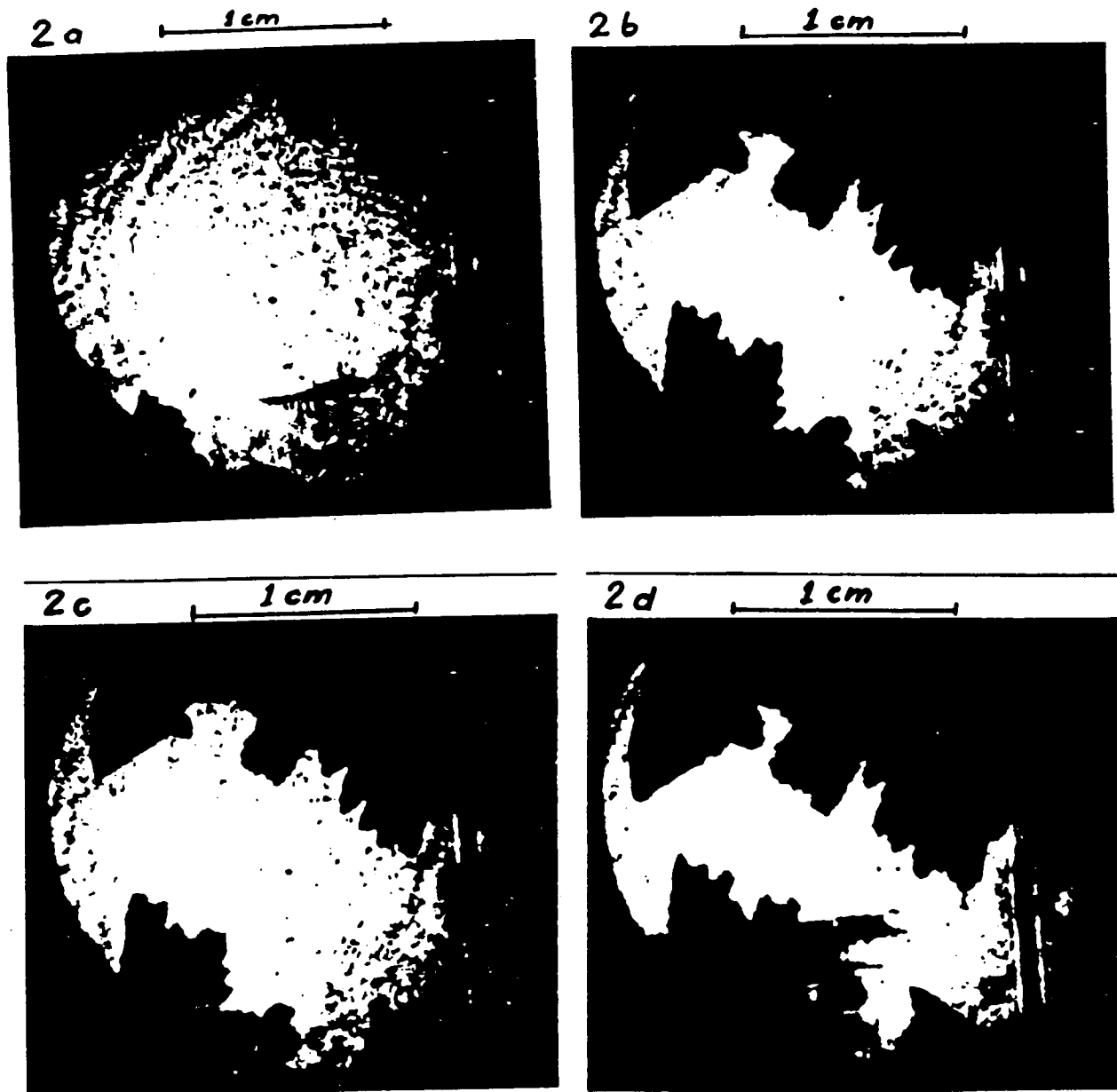


Figure 2. Shadowgraphs of solidifying KCl-LiCl eutectic melt. Chill placed beyond field of view to the right. Time of photograph reported in minutes from beginning of experiment: (a) 23, (b) 24.17, (c) 25.75, and (d) 28.67.

effect begins to dominate. This is evident in the "plumes" of the schlieren and shadowgraph images in Figure 5.

## Conclusions

Molten salts have attributes that make them attractive as physical models in solidification studies. With optical techniques of investigation such as schlieren imaging it is possible to study fluid flow phenomena in molten salts and to watch the trajectory of the solid-liquid interface. Experiments are continuing.

ORIGINAL PAGE IS  
OF POOR QUALITY.

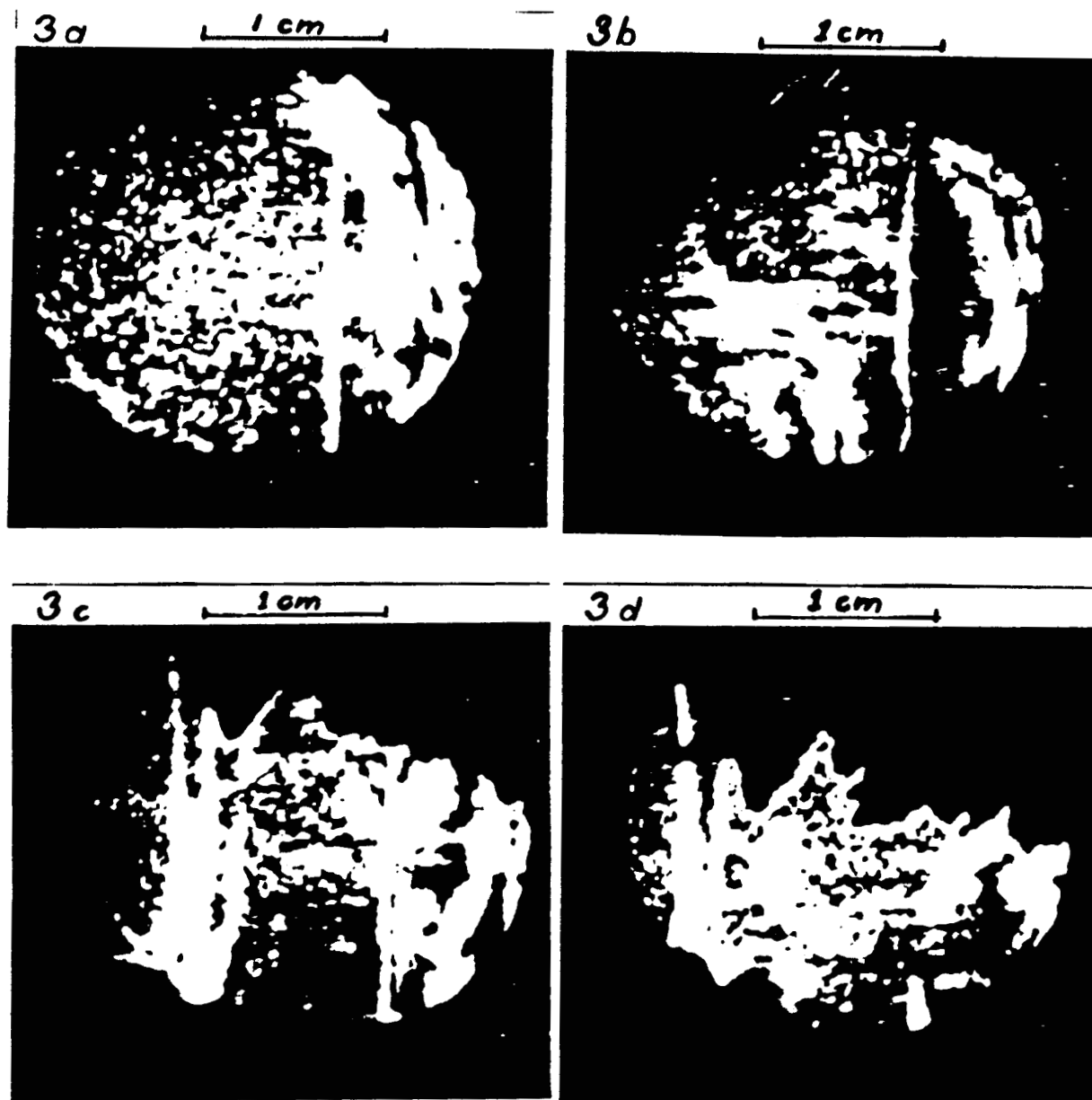


Figure 3. Schlieren images of solidifying eutectic melt. Chill placed beyond field of view to the right. Time of photograph reported in minutes from beginning of experiment: (a) 6, (b) 17.5, (c) 20.33, and (d) 24.5.

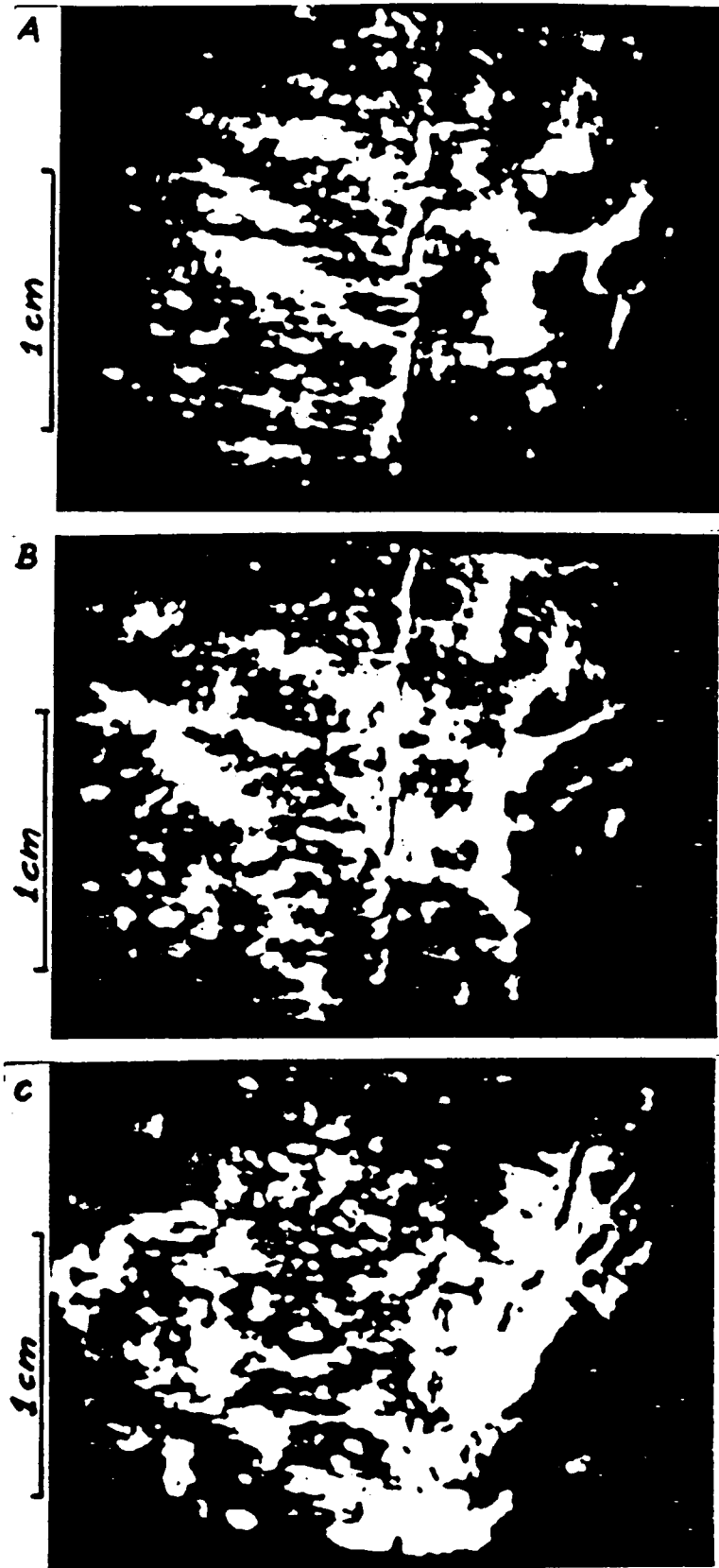


Figure 4. Schlieren images of solidifying off-eutectic (LiCl - 46.2mol% KCl) melt. Chilled from the righthand side. Visible distorted image of reference wire. Time of photograph reported in minutes from beginning of experiment: (a) 10.08, (b) 11.17, and (c) 15.42.

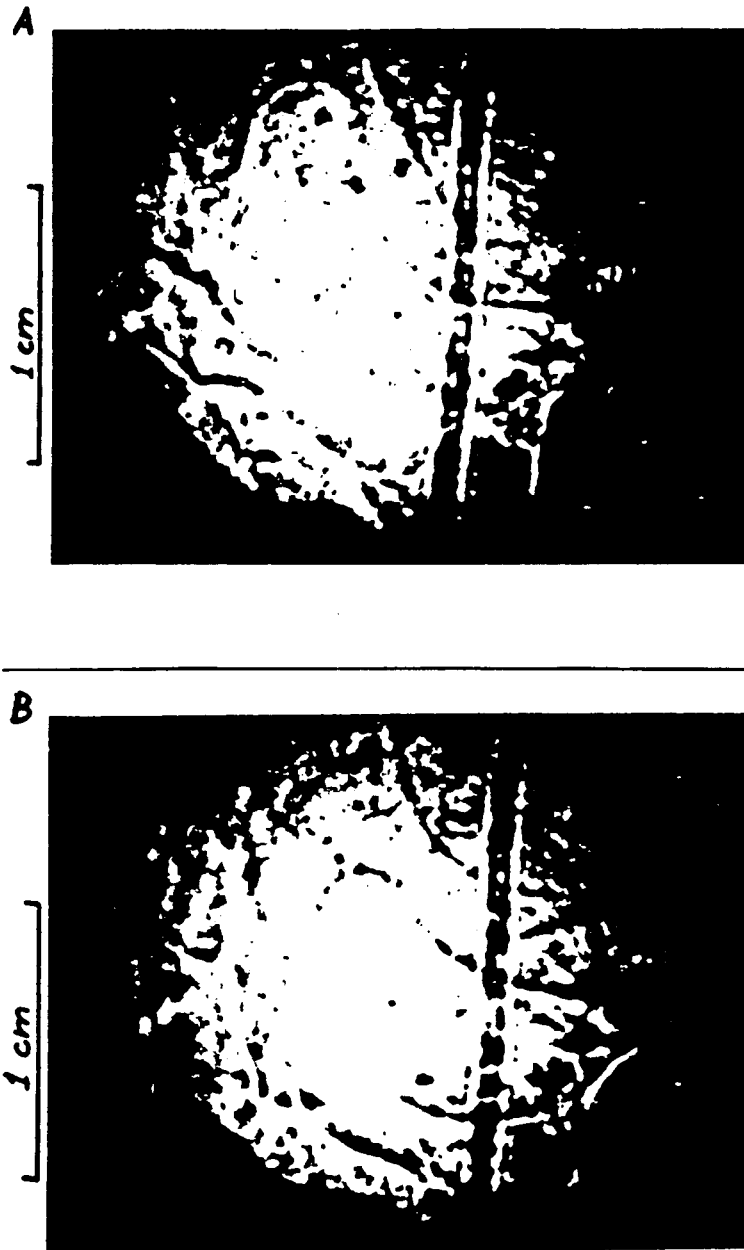


Figure 5. Shadowgraph of solidifying off-eutectic melt. Visible rising plumes caused by double diffusive phenomena. Chill placed beyond field of view to the right. Time of photograph reported in minutes from beginning of experiment: (a) 20 and (b) 20.17.

### Reference List

1. J.S. Langer, *Metall. Trans.* 15A (1984): 961.
2. M.E. Glicksman, R.J. Schaefer, and J.D. Ayers, *Metall. Trans.* 7A (1976): 1747.
3. S.R. Coriell, M.R. Coreles, W.J. Boettinger, and R.F. Sekerka, *J. Crystal Growth* 49 (1980): 13-28.